Polymer 49 (2008) 5045–5052

Contents lists available at ScienceDirect

Polymer

journal homepage: www.elsevier.com/locate/polymer

Morphology of poly[(*t*-butyl acrylate)-*b*-styrene-*b*-isobutylene-*b*-styrene-*b*-(*t*-butyl acrylate)] pentablock terpolymers and their thermal conversion to the acrylic acid form

James G. Kopchick, Robson F. Storey, William L. Jarrett, Kenneth A. Mauritz*

Department of Polymer Science, The University of Southern Mississippi, Hattiesburg, MS 39406-0076, United States

ARTICLE INFO

Article history:
Received 31 January 2007
Received in revised form 17 August 2008
Accepted 21 August 2008
Available online 6 September 2008

Keywords:
Acrylic acid–styrene–isobutylene–styrene–isobutylene–acrylic acid
Beta scission
Morphology

ABSTRACT

The morphology of a synthesized poly[(*tert*-butyl acrylate)-*b*-styrene-*b*-isobutylene-*b*-styrene-(*tert*-butyl acrylate)] pentablock terpolymer was determined using transmission electron microscopy, atomic force microscopy and small angle X-ray scattering methods. The outer blocks of this material were converted to the acrylic acid form by a thermal process that caused a beta-scission reaction in a simple thermal process, as verified by FTIR and NMR spectroscopies as well as thermogravimetric analysis. An initial heat-vacuum treatment induced a morphology that was more disordered relative to the precursor material, but when these samples were recast in THF solvent and annealed again, a considerably more refined and ordered morphology consisting of hexagonally packed cylinders resulted. This simple heat treatment allows for the *tert*-butyl groups to be converted to acrylic acid groups without dissolving the polymer or further sample cleaning. A dynamic mechanical investigation of the PtBuA form revealed three or two relaxation features depending interpretations based on the presence of three-phase morphology or a two-phase morphology in which there are mixed hard block domains.

1. Introduction

The phase separated morphologies of A–B diblock and symmetric A–B–A tri-block copolymers, where A is the minor phase of polystyrene (PS) composition and B is a rubbery block, usually have the geometrical progression spheres → rods → lamellae with increasing A block volume fraction, f_A. The particular equilibrium morphology also depends on the total copolymer molecular weight, the interaction parameter, χ_{AB}, for the dissimilar blocks, as well as f_A [1]. For solution cast materials, morphology is also influenced by solvent type, casting conditions and annealing time and temperature. When these block copolymers are melt-processed, the variables of temperature, pressure, time and rheology are important. Thermal history is important as this factor influences whether the morphology is that of the equilibrium state or is kinetically controlled if the rate of cooling is too high for equilibrium to be achieved within the time scale of the experiment.

Compared to di- and tri–block copolymers, the morphologies of triblock (A–B–C) terpolymers are more complex with more possibilities and the nature of phase separation is driven by three interaction parameters rather then one: χ_{AB}, χ_{BC}, and χ_{CA}, as well as by the particular block sequence. These morphologies have been classified and are depicted in the literature of Bates and Fredrickson [2] and Zheng and Wang [3]. Within the realm of the latter more complex materials, this paper describes studies of a new synthesized pentablock terpolymer, poly[(*tert*-butyl acrylate)-*b*-styrene-*b*-isobutylene-*b*-styrene-(*tert*-butyl acrylate)] (P*t*BuA–PS–PIB–PS–P*t*BuA) that was converted to having acrylic acid end block functionality by thermal–chemical means. The film formation conditions and morphological and spectroscopic characterizations of these materials will be described herein.

Relevant to the work reported here is our former investigations of the morphologies of synthesized poly[acrylic acid-*b*-styrene-*b*-isobutylene-*b*-styrene-*b*-acrylic acid] polymers using TEM, AFM, SAXS, and indirectly by dynamic mechanical analysis and degree of water sorption [4]. Contrasted with the present work, the *tert*-butyl acrylate end blocks in these former materials were hydrolyzed in the usual fashion. These materials possess considerable order within three-phase morphologies that contain the usual elements of rods and lamellae that are arranged as a function of polyacrylic acid block composition in continuous polyisobutylene phases

* Corresponding author. Department of Polymer Science, The University of Southern Mississippi, S.S. Box 10076, Hattiesburg, MS 39406-0076, United States. Tel.: +1 601 266 5595; fax: +1 601 266 5504.
E-mail address: Kenneth.mauritz@usm.edu (K.A. Mauritz).

0032-3861/$ – see front matter © 2008 Elsevier Ltd. All rights reserved.
doi:10.1016/j.polymer.2008.08.045

although there is a degree of uncertainty as to the exact tri-phasic morphologies for some compositions.

For the purpose of comparison, it is mentioned that solution-cast films of simpler PS–PIB–PS materials synthesized in our laboratory with 30 mass percent PS, form cylindrical morphologies, based on SAXS, TEM and AFM investigations and this morphology persists but is disrupted with PS block sulfonation as described in earlier reports [5,6].

While the work reported here deals with precursor materials with interesting structures, the ultimate goal is to generate multi-functional molecular permselective membranes, in particular those with tailored diffusion pathways due to highly articulated phase separated morphologies. One of the pathways is expected to be hydrophilic or ionophilic in nature. In the interest of efficiently generating poly(acrylic acid) (PAA) blocks in pre-synthesized P*t*BuA–PS–PIB–PS–P*t*BuA pentablock terpolymers, a thermal conversion process was explored and is described here. The two pentablocks used in this study are shown in Fig. 1. Pentablock terpolymers containing *t*BuA groups can undergo chemical hydrolysis in the typical procedure to yield acrylic acid groups. For this particular polymer, this has been accomplished in earlier studies by placing samples in 1,4-dioxane and concentrated HCl for 3 h at 80 °C [4]. The alternate process described here is neither chemically intensive nor difficult, but the polymer must be dissolved, reacted, cleaned, and dried before further use.

In particular the technique described herein that yields a similar result is performed with the simple addition of heat that causes a beta-type scission reaction that allows for the *tert*-butyl groups to be converted to acrylic acid groups without dissolving the polymer or further sample clean-up. Also, the process opens up the possibility of further morphological variation.

1.1. Block copolymer synthesis and experimental procedures

1.1.1. Materials

The pentablock terpolymer materials were produced by sequential addition of the monomers from a small molecule of 5-*tert*-butyl-1,3-bis(2-chloro-2-propyl) benzene starting with isobutylene followed by the addition of styrene. Using the Cl-terminated polymer, atom transfer radical polymerization was conducted to add *tert*-butyl acrylate. The detailed synthesis of these P*t*BuA–PS–PIB–PS–P*t*BuA triblock terpolymers is described by Storey et al. [7].

These triblock terpolymers had an average $M_n = 41{,}500$ g/mol with a polydispersity index (PDI) = 1.42. The isobutylene and styrene contents were 53% and 14%, respectively, so that the largest block fraction formed an elastomeric phase. The PAA or P*t*BuA outer blocks constituted approximately 33% of the polymer based on X_n.

1.1.2. Film casting and annealing procedures

P*t*BuA–PS–PIB–PS–P*t*BuA materials were cast from approximately 10% (w/v) solutions using THF solvent (99.9%, Fisher Co.). Solutions were poured into Teflon™ pans and tightly covered with aluminum foil in which several holes were punched with a 27G-syringe needle to allow for slow vapor release and better film formation. Films were formed over a period of 6–8 d at 60 °C and then vacuum-*annealed* for 2 d at 100–110 °C. After the solvent was driven off, the films were transparent. However, after annealing at high temperature (130 °C) under vacuum, the films were observed to contain bubbles.

1.1.3. Thermogravimetric analysis (TGA)

TGA studies were conducted on these materials using a Mettler thermal analysis workstation equipped with a TGA 850 unit. Sample sizes that were 10–15 mg were heated under 25 ml/min of nitrogen from 30 to 800 °C at a rate of 10 °C/min in alumina crucibles with and without lids.

1.1.4. Infrared spectroscopy (IR)

The FTIR/ATR apparatus that was used to verify the desired reactions was a SensIR 3-reflection horizontal attenuated total reflectance module connected to a Bruker Equinox 55 FTIR bench. The ATR module contained a composite ZnSe/diamond crystal fixed at an angle of 45°.

1.1.5. Dynamic mechanical analysis (DMA)

DMA studies were conducted on these materials using a Thermal Analysis Q800 system in tensile mode using strain control with an amplitude of 20 μm and frequency of 1 Hz with a temperature ramp of −90 up to 150 °C.

1.1.6. Transmission electron microscopy (TEM)

Specimens were prepared for TEM inspection by cryo-sectioning at an angle of 6° relative to the knife at a speed of 1.5–3.5 mm/s on a Reichard-Jung Ultracut E microtome. The microtome chamber, diamond knife, and samples were kept at temperatures between −90 and −120 °C. Ultrathin sections approximately 70 nm thick were placed on copper TEM grids. The specimens were stained with RuO_4 vapor in a Petri dish for 4 min to provide contrast for imaging the microphase separated morphology. The sections were viewed using a Zeiss EM 109-T electron microscope operating at 80 kV.

1.1.7. Atomic force microscopy

Tapping mode-phase AFM was performed using a Digital Dimension 3000 Nanoscope IIIa instrument. Tapping/phase is particularly appropriate as this mode interrogates morphology on the basis of local viscoelastic properties (i.e., hard vs. soft regions).

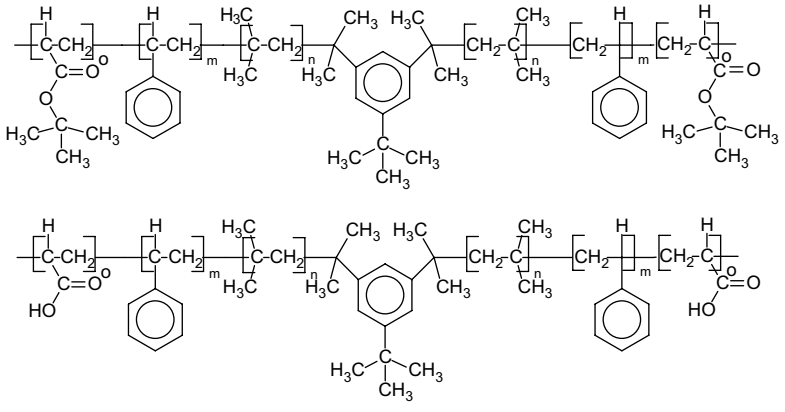

Fig. 1. Pentablock terpolymers of P*t*BuA–PS–PIB–PS–P*t*BuA (top) and PAA–PS–PIB–PS–PAA (bottom).

The scan rate was approximately 1 Hz or less. In order to minimize artifacts, all bulk sample surfaces were smoothed using a diamond knife prior to acquiring the phase images. Tapping mode was used to preserve the surface topography of the sample so that the results were reproducible.

1.1.8. Small angle X-ray scattering (SAXS) analysis

Specimens were probed by SAXS at the National Synchroton Light Source at Brookhaven National Laboratory. The system used was beam line X3A2 with a camera length = 180.1 cm and the X-ray wavelength was 1.55 Å. Scattered intensity vs. q (scattering vector magnitude) profiles were generated to provide another view of morphological order and characteristic phase spacings, $d = 2\pi/q$, where q is a peak maximum position.

1.1.9. ^{13}C solid-state nuclear magnetic resonance (SSNMR) spectroscopy

SSNMR spectroscopic analyses were performed using a Varian ^{UNITY}INOVA 400 spectrometer using a Chemagnetics three channel 4 mm PENCILÔ-style probe. Samples were loaded into zirconia rotor sleeves, sealed with Teflon™ caps, and spun at a rate of 7.0 kHz. The standard cross-polarization/magic angle spinning (CP/MAS) technique was used with high-power proton decoupling implemented during data acquisition [8]. The acquisition parameters were as follows. The ^1H 90° pulse width was 3.5 ms, the cross-polarization contact time was 1 ms, the dead time delay was 6.4 ms, and the acquisition time was 45 ms. A recycle delay of 3 s between scans was utilized, and the ^1H decoupling field of 100 kHz was implemented during acquisition.

2. Results and discussion

The P*t*BuA–PS–PIB–PS–P*t*BuA material was brittle before vacuum-annealing and broke quite easily upon handling. However, after annealing, the polymer became flexible, changed color, and became difficult to dissolve in common solvents.

A reaction of *t*-butyl groups is believed to follow a beta-type scission as depicted in Fig. 2, as will be discussed in this report. P*t*BuA homopolymer is known to undergo scission with the addition of heat + vacuum to yield acrylic acid functionalities wherein the ether and *t*-butyl groups go through this rearrangement [9]. A somewhat similar block copolymer, polystyrene-*b*-poly(1,2-butadiene)-*b*-poly(*tert*-butyl methacrylate) having different degrees of hydrolysis that were affected in the usual way (hydrolysis in a mixture of dioxane and concentrated aqueous HCl) was studied by Jiang et al. who characterized their morphologies and infrared spectroscopic features [10]. Conversion of the third block to COOH functionality was seen to cause a change the morphology.

2.1. Thermogravimetric analysis (TGA)

The thermal degradation profile of a P*t*BuA–PS–PIB–PS–P*t*BuA sample that is seen in Fig. 3 shows a sharp approximately 22% weight loss event that takes place at 233 °C. This loss is in fact close to the weight of the *tert*-butyl groups which theoretically constitute 21% of the weight of the entire polymer composition. This loss is occasionally accompanied by violent off-gassing that produces

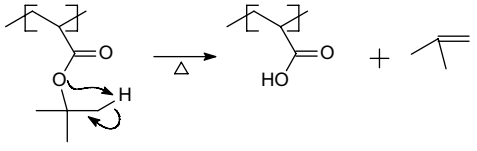

Fig. 2. Mechanism of thermal conversion of *t*BuA groups to acrylic acid groups.

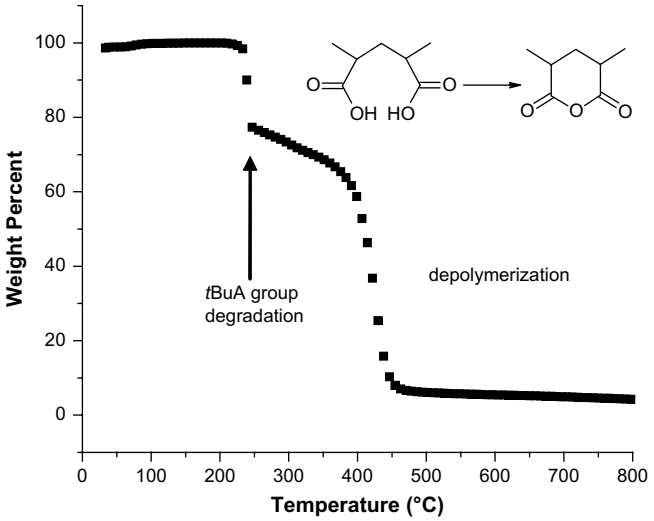

Fig. 3. TGA degradation profile of P*t*BuA–PS–PIB–PS–P*t*BuA. Chemical reaction events on the curve are indicated.

variation in the data. The second weight loss step of ~36% starting at 233 °C might involve the release of residual H_2O from the polymer due to OH groups that combine to form a 6-member cyclic ring [6] as well as chain degradation. During the second loss step, cross-links can form rather than anhydride formation. This process is not favorable, but possible nevertheless.

2.1.1. FTIR/ATR spectroscopy

The FTIR spectra of the samples, seen in Fig. 4, illustrate that significant chemical changes occur during the heat-vacuum treatment. The bands of interest are at 1150 and 1728 cm^{-1}, and in the region 2400–3400 cm^{-1} as they are signatures of *t*-butyl acrylate group scission. Scission of *t*-butyl acrylate groups creates acrylic acid groups, the evidence for which is an increase in absorbance in the region for O–H bond stretching vibrations in acrylic acid groups and the fact that the carbonyl peak shifts from 1728 to 1710 cm^{-1}. In the report of Jiang et al. dealing with similar polystyrene-*block*-poly(1,2-butadiene)-*block*-poly(*tert*-butyl methacrylate) triblock

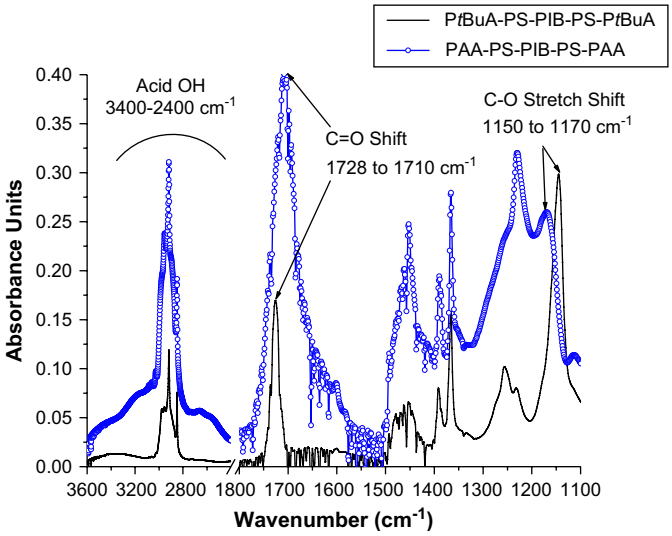

Fig. 4. FTIR/ATR spectra before and after the beta-type scission reaction: absorbance increases in the range 3400–2400 cm^{-1} by generation of COOH groups; C=O band shifts from 1728 to 1710 cm^{-1}; C–O band shifts from 1150 to 1170 cm^{-1}.

copolymers a band at 1725 cm^{-1} was noted and was assigned to the carbonyl group [10].

Also, there is a shift in the C–O stretching signal from 1150 to 1170 cm^{-1}. These results show that scission occurred, but it is not certain from this analysis that all *tert*-butyl groups were cleaved in this way.

Ring C=C peaks in benzene and substituted benzene can vary over a considerable range 1650–1450 cm^{-1} [11]. The spectrum of toluene shows absorptions in the regions 1600–1585 cm^{-1} and 1500–1400 cm^{-1} due to carbon–carbon stretching vibrations in the aromatic ring. In the spectra in Fig. 4, absorbances seen in the low wave number region of this range could be assigned to C=C stretching.

2.1.2. Solid state NMR (SSNMR) spectroscopy

Nonetheless, it is important to confirm whether full or partial *t*BuA group scission occurred. ^{13}C SSNMR spectroscopy was used to answer this because of the inability of the pentablock material to dissolve in common deuterated solvents for a lock on the signal. This insolubility problem was the same as that for the case where *t*BuA groups were hydrolyzed to acrylic acid.

Simulations of the NMR spectrum using model compounds were conducted to predict the conversion from P*t*BuA to PAA outer blocks. The predictions were created using ChemDraw Ultra 7 software which calculates chemical shift changes affected by directly attached functional groups. The prediction was generated by using a simple base molecule and adding the amount of shift normally associated with the functional groups attached to the base.

A simple small molecule homologue consisting of (*tert*-butyl acrylate)–styrene–isobutylene predicts the position of the carbonyl group at 172 ppm while the *tert*-butyl methyl group is at 29 ppm. A small molecule homologue of (acrylic acid)–styrene–isobutylene predicts the disappearance of the *tert*-butyl methyl groups at 29 ppm and a carbonyl peak shift from 172 ppm to 177 ppm.

Experimental SSNMR spectra were similar to those predicted by the model compound calculations. A spectrum of P*t*BuA–PS–PIB–PS–P*t*BuA is shown in Fig. 5. The carbons in the phenyl ring are difficult to determine in ^{13}C SSNMR spectra as all the peaks are broadened due to low chain mobility in these hard blocks. The *tert*-butyl methyl peak, labeled h, can clearly be seen as well as the carbonyl peak, labeled f. All other unlabeled peaks in this spectrum are spinning sideband artifacts, which is a byproduct of this solid state NMR procedure.

An NMR spectrum of PAA–PS–PIB–PS–PAA produced by chemical hydrolysis is shown in Fig. 6. The methyl group carbon peak of *tert*-butyl (h) at 29 ppm is no longer seen while the carbonyl peak (f) that was near 175 ppm shifts to 180 ppm. The quaternary carbon of the *tert*-butyl group (g) present at 80 ppm disappears as the material is hydrolyzed. The unhydrolyzed and hydrolyzed sample spectra are shown together in Fig. 7. As mentioned, all other peaks in this spectrum are spinning sideband artifacts. Due to the nature of this test, peaks cannot be integrated to offer more qualitative information on composition. Nonetheless, the disappearance of *tert*-butyl groups is the result of significance.

Having established that ^{13}C SSNMR spectroscopy is capable of verifying conversion to COOH groups in the outer blocks by chemical hydrolysis, the samples that were converted to the acrylic acid form with the addition of heat + vacuum were then analyzed. The spectrum of a heat + vacuum-reduced sample, as well as that of a chemically hydrolyzed sample, is shown in Fig. 8. Again, the size and height of the peaks do not allow for deriving quantitative compositions. However, if any *t*BuA groups remained, this technique would be capable of distinguishing them with an error of 5–10%. As seen in Fig. 8, the sample that underwent heat-vacuum treatment shows full reaction according to the NMR spectrum. As mentioned, TGA indicated a 25% weight loss at 233 °C, which is consistent with the conversion of the end blocks from P*t*BuA to PAA functionality.

P*t*BuA–PS–PIB–PS–P*t*BuA was heated with no vacuum at 250 °C for 15 min. Fig. 9 clearly indicates two carbonyl signals; however, the methyl group carbon peak for the *tert*-butyl group at 29 ppm is no longer seen. This indicates full conversion, while the lower carbonyl peak is most likely due to formation of the anhydride ring with the carbonyl predicted to shift to 171 ppm by the use of ChemDraw Ultra 7 software.

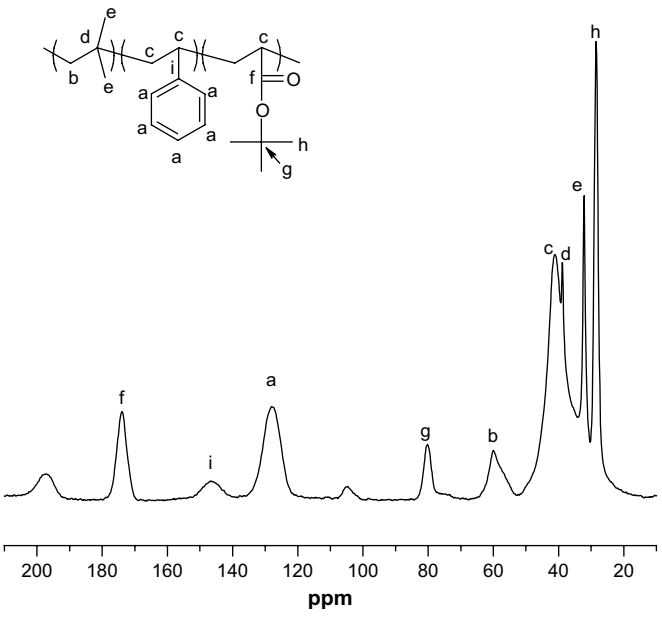

Fig. 5. ^{13}C SSNMR spectrum of unmodified P*t*BuA–PS–PIB–PS–P*t*BuA showing peak assignments.

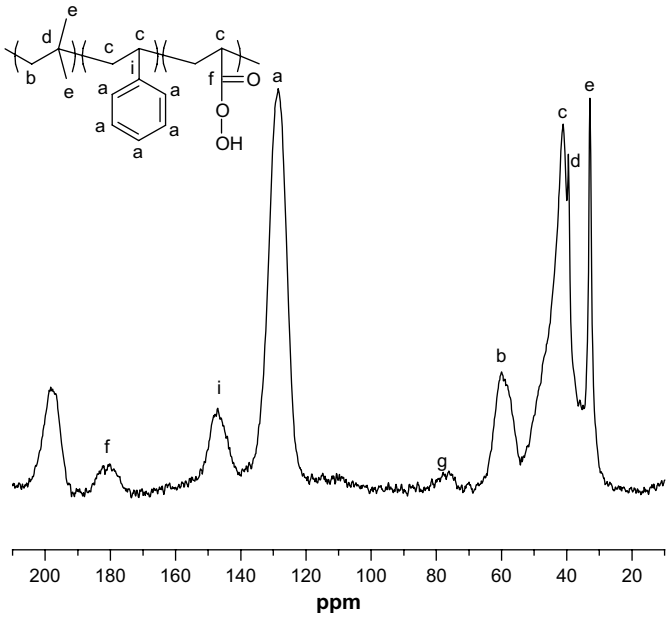

Fig. 6. ^{13}C SSNMR spectrum of heat-vacuum produced PAA–PS–PIB–PS–PAA showing peak assignments.

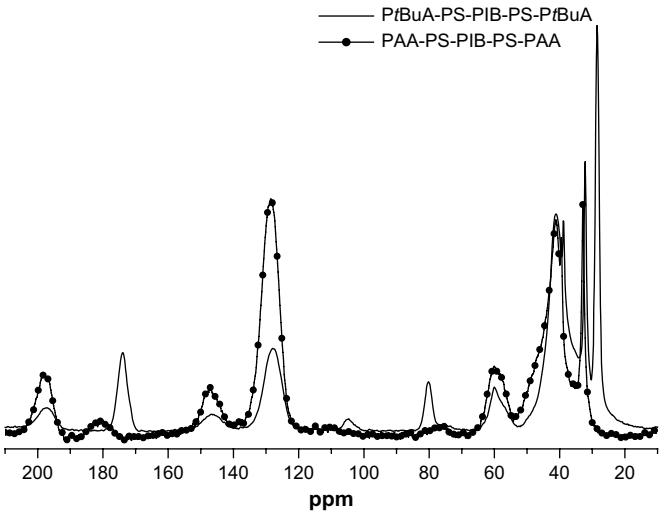

Fig. 7. ^{13}C SSNMR spectra of P*t*BuA–PS–PAA–PS–P*t*BuA and PAA–PS–PIB–PS–PAA produced with chemical hydrolysis.

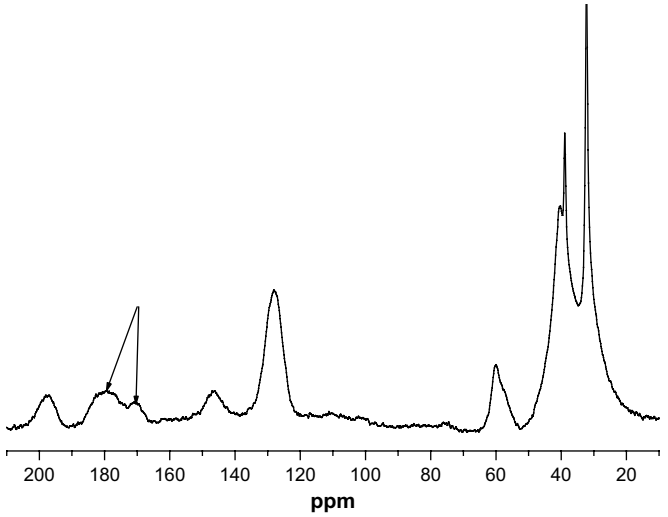

Fig. 9. ^{13}C SSNMR spectrum that shows full P*t*BuA scission with anhydride ring formation.

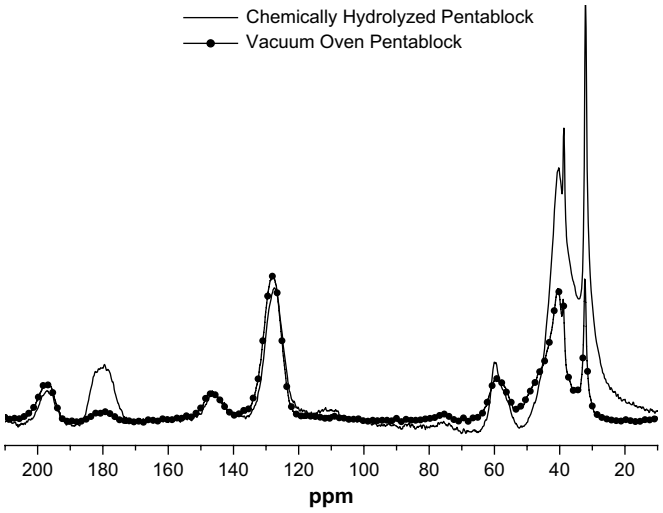

Fig. 8. Comparison of the ^{13}C SSNMR spectrum of a chemically-hydrolyzed pentablock terpolymer with the spectrum of a corresponding sample that underwent beta-type scission by heat to generate PAA end blocks.

2.1.3. Dynamic mechanical analysis (DMA)

Fig. 10(a) illustrates the tan δ vs. temperature (T) plot for the pentablock terpolymer before the treatment that leads to the scission reaction, as well as the corresponding storage modulus (E') vs. T plot. The plot shows three relaxation processes which suggest a phase separated morphology. It is logical to assign the low temperature relaxation to the glass transition of the PIB phase. This relaxation feature appears to have a high temperature shoulder that might be assigned to sub-Rouse motions as in the cases of the earlier-studied PS–PIB–PS triblock copolymers [12].

There is a well-defined peak at around 50 °C that must be the glass transition of either the P*t*BuA or PS block phase or the glass transition of a mixed P*t*BuA + PS phase. The E' vs. T graph shows the step decreases for all relaxations. The terminal softening at the highest temperature occurs at around 100 °C. T_g for pure P*t*BuA can range from as low as 43–107 °C while that for pure PS is 100 °C [13]. For this reason, as well as the fact that the P*t*BuA block composition is high at 33% by weight, it might be considered that the strong peak at ~50 °C is the signature of the *tert*-butyl acrylate block domain glass transition. This would be the case if the relaxation activity near 100 °C is due to the PS block phase that underwent a glass transition shortly after which the material can immediately flow since the PS block composition is low, at ~14% by weight. Assuming the validity of these relaxation assignments, DMA indicates the presence of three phases. On the other hand, if there are only two phases, namely the soft PIB and a mixed P*t*BuA/PS phase, the high temperature event might simply be material flow owing to a greatly decreased viscosity at around 100 °C.

In addition to block composition and block length, T_g of a given phase is expected to be influenced by block sequence and phase geometry especially for short block lengths.

While these DMA results were simply meant to identify the relaxation characteristics of the precursor material, and implications with regard to morphology, future studies will involve materials that have been thermally converted to the PAA end block form and these results will be reported in detail.

3. TEM and AFM

^{13}C SSNMR spectroscopy suggests that the degree of conversion to the acid form is ~100%, although there can be a 5–10% error in

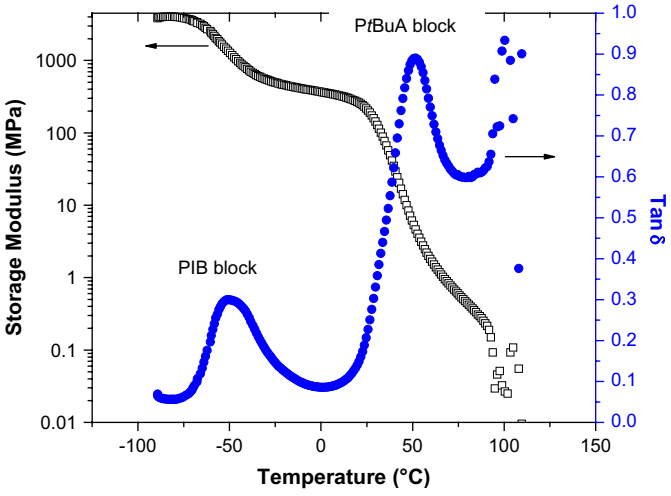

Fig. 10. tan δ and dynamic storage modulus (E') vs. T for the unmodified pentablock terpolymer.

this number. Perhaps, due to the reaction plus the weight loss that occurs during annealing, this sample may not have had time to reach equilibrium morphology. This possibility must be considered when viewing the microscopic images that will be presented here.

Tapping/phase AFM images of P*t*BuA–PS–PIB–PS–P*t*BuA before the heat-vacuum treatment are shown in Fig. 11 and a TEM image of the same sample is displayed in Fig. 12. The AFM images clearly show phase separation, although assignment of block composition to the features is not possible given this coarse level of morphological refinement and resolution. Somewhat of a lamellar structure is seen in the lower image, although further evidence is needed for verification. Inter-domain spacing on these images is in the range 30–35 nm. The TEM image also shows phase separation in periodic striations but the contrast variation and morphological refinement is insufficient for assigning particular block compositions to different regions. Inter-feature spacing taken from this TEM image is in the range of 25–35 nm which is in approximate agreement with the inter-domain spacing in the AFM image. It is seen, in the lower portion of the TEM image, that spacing is lesser than in the upper portion. Perhaps this is an effect due to lamellar planes being oriented at different angles so that one is viewing the projection of the layering in the plane of the image.

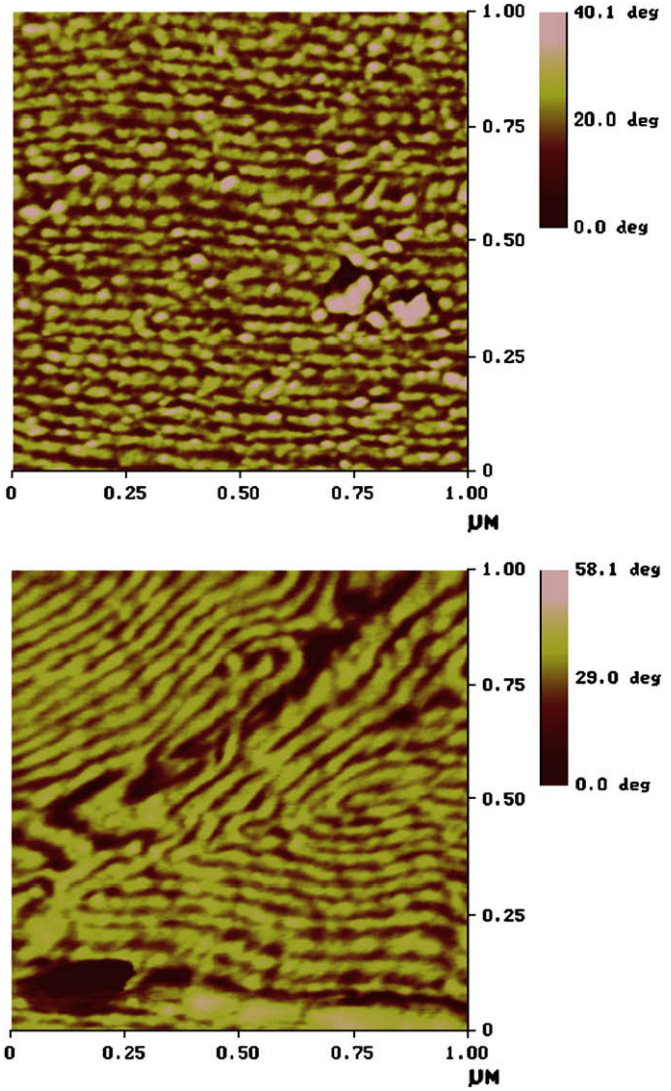

Fig. 11. AFM tapping/phase images of two different regions on the microtomed surface of a P*t*BuA–PS–PIB–PS–P*t*BuA sample before the heat-vacuum treatment.

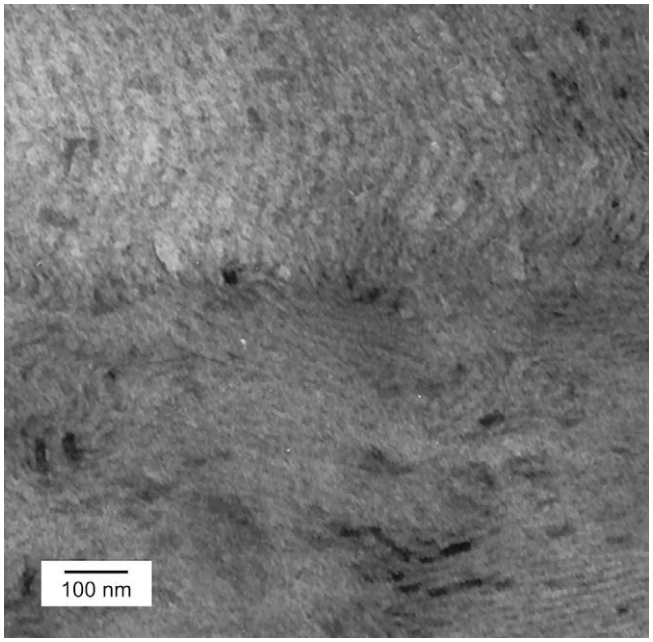

Fig. 12. TEM micrograph of a P*t*BuA–PS–PIB–PS–P*t*BuA sample before heat-vacuum treatment (same sample whose AFM image is Fig. 11).

An AFM tapping/phase image of the heat + vacuum induced PAA–PS–PIB–PS–PAA morphology is seen in Fig. 13. This image is quite different from those in Figs. 11 and 12 and shows small hard features of circular crosssections of dimensions of 12–40 nm that are most likely PS and PAA–rich domains. This is reasonable also because the PIB blocks would constitute the major continuous phase in this polymer (53%), which are the darker regions, whereas the PAA composition was 33%. Perhaps the small circular areas are PS, because these blocks have only 14% composition and the undefined hard areas are of PAA composition. This poorly formed phase separated morphology is likely not of an equilibrium nature. This condition could be caused by the retarding influences of concurrent chemical reactions, intermolecular hydrogen bonding interactions between introduced COOH groups and reaction

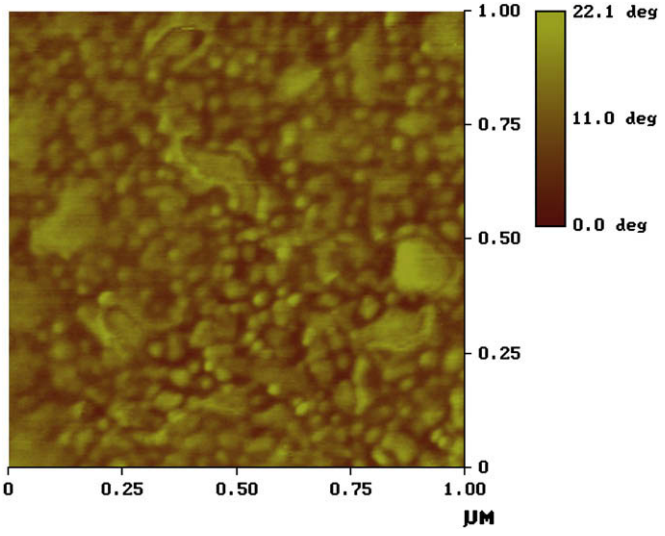

Fig. 13. AFM tapping/phase image of the morphology of a P*t*BuA–PS–PIB–PS–P*t*BuA sample that was annealed under vacuum and the outer blocks transformed formed into PAA composition.

by-product mass loss on the dynamics of chain organization into a complex morphology within the experimental time frame of the heat-vacuum treatment.

TEM studies of the same heat-vacuum treated sample were conducted and morphology similar to that shown by AFM is seen in Fig. 14. The PAA blocks are thought to form the larger domains, while the minor PS phase assumedly takes the form of an array of spherical particles. There are two types of spherical objects in Fig. 14. The darkest objects are less than 50 nm in size and since the PS blocks will absorb this particular staining agent more efficiently than the PAA blocks, they are reasonably assigned to be of PS composition. However, some spheres are light gray which may suggest that these are of PAA composition. Or, all of the spheres may be of PS composition with those near the surface absorbing the staining agent more effectively.

In a final step, these same PAA–PS–PIB–PS–PAA samples were recast in THF solution and likewise annealed again. This treatment produced a considerably more refined and more ordered morphology that consists of hexagonally packed cylinders as shown in Fig. 15. Perhaps the shift from lamellae to cylinders – with the intervening frustrated morphology – was caused by the 22 wt% mass loss from the outer blocks so as to give a lower volume fraction for this phase. The axes of these cylinders are spaced by ~25–35 nm. No clearly defined third phase is apparent given the quality of microscopic resolution. It was mentioned that the morphologies of a series of essentially the same P(*t*-BuA)–PS–PIB–PS–P(*t*-BuA) pentablock terpolymers – but for which the outer blocks were converted into PAA blocks by the usual chemical hydrolysis procedure – were reported. The micrograph for a sample from this series, that has a somewhat different block composition (50% PIB/26% PS/24% PAA) and chemical history, shows what are likely PAA cylinders within cylinders of PS [4].

It might be considered that the PAA phase also has anhydride groups present although these groups would be unstable in the presence of water. In any case, if the PAA phase elements were reasonably contiguous, water could diffuse throughout and open the anhydride rings.

The microscopy studies were complemented with SAXS investigations of morphology. Scattered intensity vs. q profiles and the Bragg spacings associated with peak maxima are shown in Figs. 16 and 17 for both the P*t*BuA–PS–PIB–PS–P*t*BuA and the PAA–PS–PIB–PS–PAA materials that were subjected to the second annealing process that produced the well-defined hexagonal cylinder packing seen in Fig. 15.

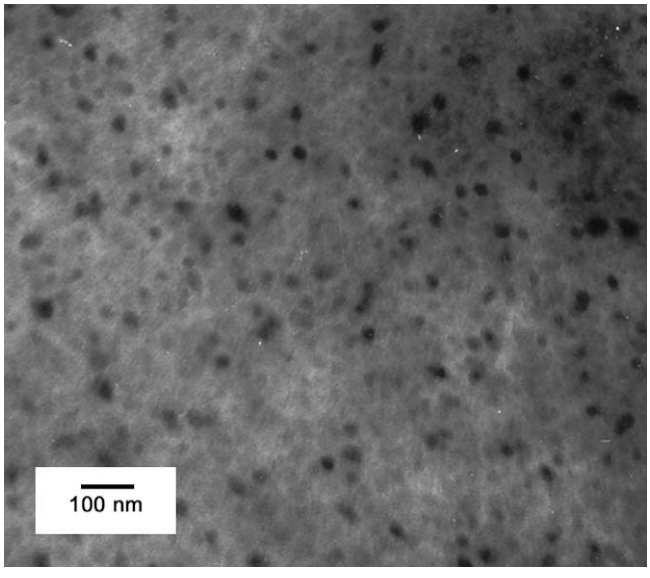

Fig. 14. TEM micrograph of a stained P*t*BuA–PS–PIB–PS–P*t*BuA sample that was annealed under vacuum and PAA outer blocks formed. Two types of spherical domains are visible.

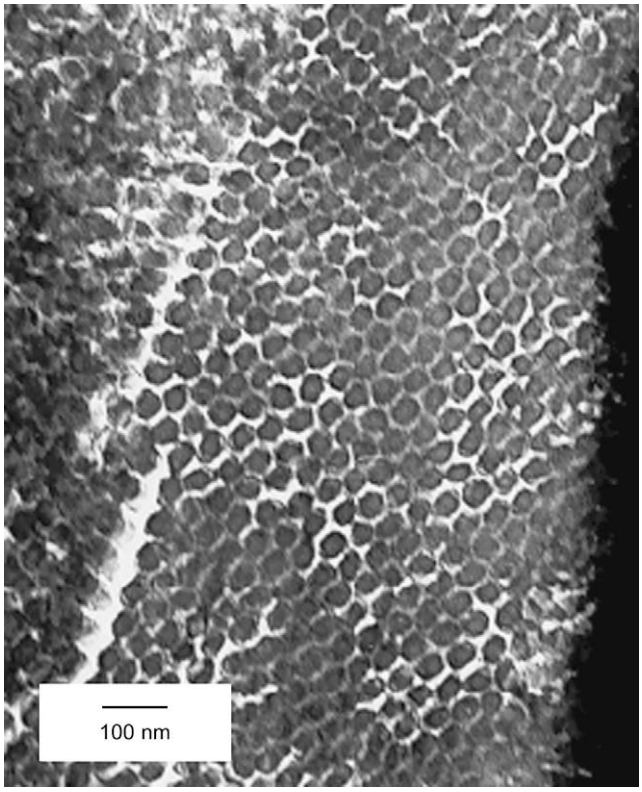

Fig. 15. TEM images of a recast and subsequently annealed PAA–PS–PIB–PS–PAA sample.

The small angle scattering intensity vs. q profile for the P*t*BuA–PS–PIB–PS–P*t*BuA precursor showed two peaks. The weak peak at the higher q value is close to the relative (q_2/q_1) location for the second peak corresponding to lamellar morphology (2.052 vs. 2.000) although there are no higher order peaks, which is also seen by the lack of rings in the 2-D scattering pattern that is an inset in Fig. 16. This reflects a lack of highly developed long range order

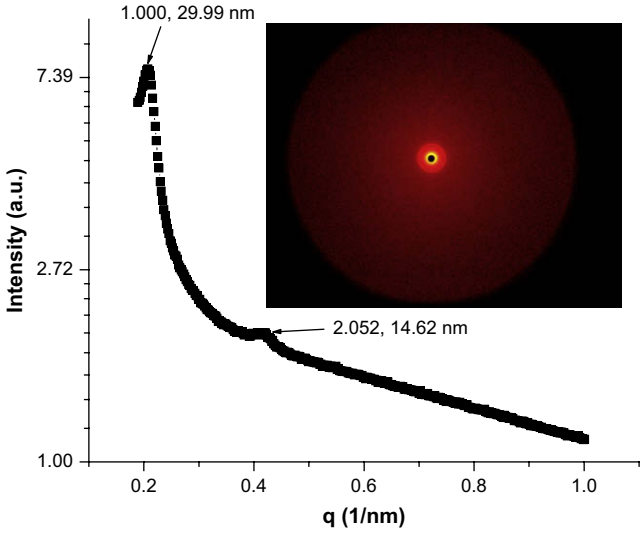

Fig. 16. SAXS scattered intensity vs. q profile and integration of an un-annealed P*t*BuA–PS–PIB–PS–P*t*BuA sample.

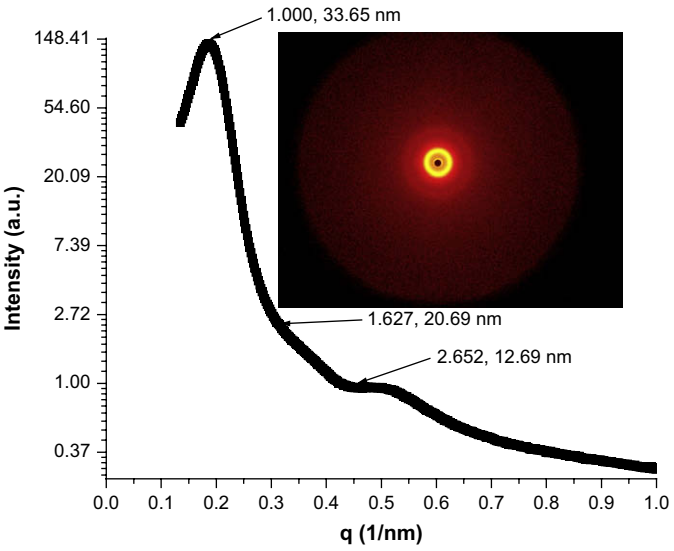

Fig. 17. SAXS intensity vs. q profile and integration for a twice-annealed PAA–PS–PIB–PS–PAA sample.

within the phase separated morphology [14,15]. These SAXS results are in good agreement with the morphology seen in both the AFM and TEM images of this polymer in Figs. 11 and 12 that also indicate poor long range ordering. Moreover, the inter-lamellar spacing measured from the TEM image (25–35 nm) and the primary Bragg spacing derived from SAXS (30 nm) are in approximate agreement.

There are three peaks on the scattering curve for the recast – then subsequently annealed PAA–PS–PIB–PS–PAA sample in Fig. 17. The relative peak position sequence is somewhat close to that for the simpler PS–(soft block)–PS triblock copolymers having hexagonal packed cylinder morphology, which, ideally, is 1, $\sqrt{2}$ (1.41), $\sqrt{3}$ (1.73), $\sqrt{7}$ (2.65). A higher degree of long range order, relative to the P*t*BuA–PS–PIB–PS–P*t*BuA precursor, is also seen in terms of the better-defined rings in the 2-D pattern that is the inset in Fig. 17, as well as in the TEM image in Fig. 15. It is possible that a third phase is contained within another phase which may not significantly alter the Bragg reflections generated by cylindrical morphology. The primary Bragg spacing obtained by SAXS (34 nm) and the inter-domain spacing measured on the TEM image (25–35 nm) are in approximate agreement.

It must be considered that heat induced anhydride formation and crosslinking reactions might occur. This leads to the question of whether chemical crosslinking or simple hydrogen bond formation would increase cohesion in the outer block phase. While it was observed that the vacuum-annealed sample of the P*t*BuA form of this polymer could readily re-dissolve, the recast sample of this material could not and this could be indirect evidence of increased cohesion in the outer block phase.

Using a similar material with a discontinuous PAA phase, the issue of increased cohesion was briefly investigated via a simple solubility test. The material had PDI = 1.31 and a total M_n of 38,500 g/mole, with the PIB, PS, and P*t*BuA blocks having M_n values of 14,700, 8300 and 15,500 g/mol, respectively. These tests imply that some sort of enhanced interaction in the outer blocks occurs due to the fact that this material would swell but not dissolve in very strong solvents including 1-methyl-2-pyrrolidinone, methyl sulfoxide, and 1,4 dioxane.

4. Conclusions

The *t*BuA groups in synthesized P*t*BuA–PS–PIB–PS–P*t*BuA pentablock terpolymers were converted to PAA groups under the influence of heat and vacuum during a simple annealing procedure at a temperature above the highest T_g of the three constituent blocks. This simple process stands in contrast with the usual chemical hydrolysis reaction. Thermogravimetric analysis, FTIR and ^{13}C SSNMR spectroscopic investigations clearly demonstrated the conversion of these materials to the acid form through a beta type scission reaction of *t*-butyl groups. Thus, samples can be simply hydrolyzed by their exposure to 100 °C at 30 mmHg of vacuum for varying times depending on sample size, or by exposure to heat above 233 °C. This process has benefits over the usual chemical hydrolysis process.

The morphology observed after a first annealing consisted of poorly developed lamellae but with further annealing and re-solution casting, a better-refined cylindrical morphology was obtained. The morphologies and characteristic spacings seen by TEM, AFM and SAXS are consistent. The morphology probed by TEM and AFM only shows 2 phases although it is possible that a third phase may reside in the cylinders.

A dynamic mechanical investigation of the P*t*BuA form revealed three relaxation features reflective of three-phase morphology. In the future, a complete analysis of heat-vacuum treated samples will be given.

There is the possibility of a crosslinking reaction which might prevent the polymer from being soluble although this may not be a problem with samples with continuous PAA phases because water can reverse the reaction. With these particular block lengths, when crosslinking and anhydride ring formation take place, the reactions would be irreversible due to the outer block phase being isolated.

Acknowledgements

R. Moore, A. Phillips, and K. Page obtained the SAXS data and A. Scheuer performed the polymer synthesis. The SAXS studies were performed at the National Synchrotron Light Source, Brookhaven National Laboratory, which is supported by the U.S. Department of Energy, Division of Materials Sciences and Division of Chemical Sciences (contract DE-AC02-98CH10886). The support of this work by the Army Research Office (DAAH04-96-1-0191) is appreciated.

References

[1] Bates FS, Fredrickson GH. Ann Rev Phys Chem 1990;41:525.
[2] Bates FS, Fredrickson GH. Phys Today 1999;52:32.
[3] Zheng W, Wang Z. Macromolecules 1995;28:7215.
[4] Kopchick JG, Storey RF, Beyer FL, Mauritz KA. Polymer 2007;48:3739.
[5] Mauritz KA, Storey RF, Mountz DA, Reuschle DA. Polymer 2002;43:4315.
[6] Mauritz KA, Storey RF, Reuschle DA, Beck Tan N. Polymer 2002;43:5949.
[7] Storey RF, Scheuer A, Achord B. Polymer 2005;46:2141.
[8] Schaefer J, Stejskal EO, Buchdahl R. Macromolecules 1977;10:384.
[9] Fernández-García M, Fuente J, Cerrada M, Madruga E. Polymer 2002;43:3173.
[10] Jiang S, Göpfert A, Abetz V. Macromolecules 2003;36:6171.
[11] Conley RT. Infrared spectroscopy. 2nd ed. Allyn and Bacon; 1972.
[12] Kwee T, Taylor SJ, Mauritz KA, Storey RF. Polymer 2005;46:4480.
[13] Brandrup J, Immergut E. Polymer handbook. 3rd ed.; 1989. p. VI209–78.
[14] Sakurai S, Momii T, Taie K, Shibayama M, Nomura S, Hashimoto T. Macromolecules 1993;26:485.
[15] Sakurai S, Kawada H, Hashimoto T, Fetters L. Macromolecules 1993;26:6525.